Exciton-state mixing effects in photoinduced intersubband transitions in quantum-well structures

Y. Chen, S. M. Sadeghi, and W. P. Huang
Department of Electrical and Computer Engineering, McMaster University, 1280 Main Street West, Hamilton, Ontario, Canada L8S 4K1

(Received 4 January 2007; revised manuscript received 12 March 2007; published 18 June 2007)

We study the effects of exciton-state mixing on photoinduced conduction intersubband transitions in undoped quantum wells. Valence-band mixing and exciton-state mixing of different orbital angular momenta (s, p, d, etc.) are fully accounted for in the analysis. We show that, when the exciton-state mixing is significant, an infrared laser near resonant with two conduction subbands in quantum wells can excite intersubband excitations with different orbital angular momentum attributions, imitating the electronic transitions in quantum dots. In other words, instead of pure electronic states, the initial and final states of such intersubband transitions become mixed excitonic states, making their dipole moments strongly dependent not only on the s component but also on p and d components. Our results show that the inclusion of all the orbital angular momenta gives accurate evaluation of the dipole moment of the photoinduced intersubband transitions, which may have been drastically overestimated by electron to electron transition model or underestimated by the exciton transition model without exciton-state mixing.

DOI: 10.1103/PhysRevB.75.233409 PACS number(s): 78.67.De, 78.66.Fd

Intersubband transitions (ISTs) between quantized states of low-dimensional quantum structures have been widely used to study numerous fundamental physical processes and to develop novel optoelectronic devices. In addition to their prime roles in understanding relaxation processes, electronic states, carrier-carrier scattering, etc., in quantum wells (QWs), wires, and dots, such transitions are particularly appealing for the investigation of coherent optical processes. Some of these effects include electromagnetically induced transparency,[1,2] coherent population trapping,[2] gain without inversion,[3] and Rabi flopping.[4] Moreover, characteristic properties, such as relaxation processes, electron-hole interaction, and carrier multiplication of nanocrystals, have been widely investigated using ISTs.[5] In terms of device applications, ISTs are the backbone of mid- and far-infrared lasers,[6] all-optical modulators,[7] detectors,[8] etc.

Most of the investigations of ISTs have been carried out either in doped (n type or p type) or undoped QWs. In n-type QWs, an infrared laser can lead to the excitation of electrons from the heavily populated conduction ground subband to an upper one. In undoped QWs, however, such a process requires simultaneous application of an interband optical field to excite electrons (and holes), causing the so-called photoinduced intersubband transitions (PI ISTs).[9] In contrast to many of the previous investigations wherein the nature of such transition was considered similar to that of the ISTs in n-doped QWs,[10] some recent studies have shown that they could be significantly different.[11,12] The main reason for this is related to the fact that PI ISTs happen in the presence of the photoexcited holes that are simultaneously generated by the interband laser field. Therefore, as shown in Ref. 12, Coulomb interaction between the photoexcited electrons and holes can drastically influence such transitions. In other words, Coulomb interaction makes PI ISTs strongly excitonic in nature, allowing them to be influenced by the spinor mixing of the valence subbands significantly.

In the previous studies, the effects of valence subband spinor mixing on PI ISTs were studied considering excitation of s-state excitons. Only the transitions between the $1s$ and $2s$ states of the excitons associated with e1 and e2 were included [Fig. 1(b)]. It is known, however, that when two valence subbands are in proximity of each other, exciton states are no longer pure, i.e., they cannot be described by a single orbital angular momentum (m). Under such a condition, the interband selection rules that only allow the formation of excitons with zero orbital angular momentum ($m=0$) are relaxed. Therefore, depending on the QW parameters, an exciton state can be a mixture of various m (s, p, d, etc.). Our objective in this Brief Report is to study how such an excitonic angular mixing process influences the PI ISTs and discuss how it can characteristically determine the physical nature of the interaction between intense infrared laser fields and undoped QWs. We show that when such a mixing process occurs, an infrared laser near resonant with e1 and e2 can, in fact, lead to intersubband excitations with different angular momentum attributions, imitating the electronic transitions in quantum dots.[13] Under this condition, the IST between e1 and e2 can be translated into transitions between s, p, or d states of the excitons associated with e1 with those of the excitons associated with e2. It will be shown in the following how the presence of non-s-state components will affect the oscillator strengths of the PI ISTs and how they can be engineered by the strain in QWs.

As demonstrated in Ref. 12, an important feature of PI ISTs in undoped QWs is that although they happen as elec-

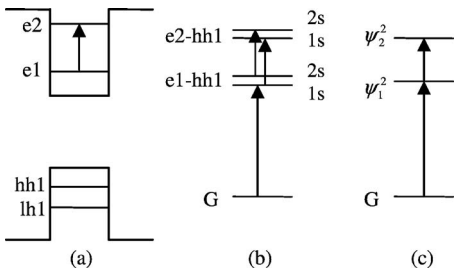

FIG. 1. Schematic diagram of the intersubband transitions in an undoped QW. (a) The electronic e1-e2 transition, (b) the transitions between pure s states of the excitons associated with e1 and e2, and (c) the transition between mixed exciton states.

trons are excited from one conduction subband (e1) to another (e2) [Fig. 1(a)], they are, in fact, the transitions between exciton states associated with these subbands [e.g., from $1s$, $2s$ of the e1-hh1 exciton to $1s$, $2s$ of the e2-hh1 exciton, Fig. 1(b)]. In Fig. 1(b), however, the exciton states are associated with only one conduction subband and one valence subband. This is valid only when the valence subbands are well separated from each other. When the valence subbands are close to each other, for instance, in the cases of wide or properly strained QWs, the exciton states associated with individual valence subbands may mix together.[14,15] In the presence of such a mixing process, the exciton states associated with the ith conduction subband is represented as[12,16]

$$\Psi_i^{\xi}(\mathbf{r_e},\mathbf{r_h}) = \sum_j \Psi_{i,j}^{\xi,\beta} = \sum_{j,\mathbf{k}} G_{i,j}^{\xi,\beta}(\mathbf{k})\phi_{i,\mathbf{k}}(\mathbf{r_e})\phi_{j,-\mathbf{k}}(\mathbf{r_h}), \quad (1)$$

where $\Psi_{i,j}^{\xi,\beta}$ is the two-band exciton state associated with the ith conduction subband and jth valence subband. ξ is the total angular momentum along the z direction (the growth direction) and β is the exciton index, i.e., $1s$, $2p$, and $3d$. The mixed exciton state Ψ_i^{ξ} is characterized by the ith conduction subband and ξ. In contrast to $\Psi_{i,j}^{\xi,\beta}$ that represents pure s states or p states and has been discussed in Ref. 12, Ψ_i^{ξ} describes mixed s, p, or d states associated with different valence subbands. Under the condition of state mixing, the PI ISTs associated with e1 and e2 [Fig. 1(a)] are, in fact, happening between mixed states associated with these two subbands, i.e., from Ψ_1^2 to Ψ_2^2 [Fig. 1(c)].

The exciton wave functions can be further written as a product of three functions such as the second term in Eq. (1). $\phi_{i,\mathbf{k}}(\mathbf{r_e})$ and $\phi_{j,-\mathbf{k}}(\mathbf{r_h})$ are the electron and hole wave functions in quantum wells without Coulomb interaction. $G_{i,j}^{\xi,\beta}(\mathbf{k})$ is the exciton-state function in momentum space that describes the relative movement between electrons and holes due to Coulomb attraction. The wave functions $\phi_{i,\mathbf{k}}(\mathbf{r_e})$ and $\phi_{j,-\mathbf{k}}(\mathbf{r_h})$ have been studied extensively before.[17] $G_{i,j}^{\xi,\beta}$ can be obtained through:[12,16]

$$[E_i^c(\mathbf{k}) + E_j^h(\mathbf{k})]G_{i,j}^{\xi,\beta}(\mathbf{k}) + \sum_{j',\mathbf{q}\neq\mathbf{0}} V_{i,jj'}(\mathbf{q})G_{i,j'}^{\xi,\beta}(\mathbf{k}+\mathbf{q}) = E_i^{\xi}G_{i,j}^{\xi,\beta}(\mathbf{k}). \quad (2)$$

Here E_i^{ξ} is the exciton transition energy and $V_{i,jj'}$ refers to the Coulomb interaction between electrons and holes. E_i^c and E_j^h are the energies of electrons and holes before Coulomb interaction is included.

To study the effects of exciton-state mixing on the PI ISTs, we need to calculate the dipole moment of PI ISTs defined as

$$\mu_{ii'}^{\xi} = e\langle\Psi_i^{\xi}|z|\Psi_{i'}^{\xi}\rangle. \quad (3)$$

In the mixed exciton states, ξ is the only well-defined quantum number. We are interested in two representative states: $\xi=2$ states and $\xi=0$ states. Using the designation introduced in Refs. 12 and 14, the $\xi=2$ state associated with conduction subband e1 ($i=1$) can be expressed as

$$\Psi_1^2 = a\Psi_{1HH_1}^{2,s} + b\Psi_{1LH_2}^{2,p+}. \quad (4)$$

It consists of s state of HH1 and p^+ state of LH2. Similarly, the $\xi=0$ state associated with e1 can be written as

$$\Psi_1^0 = a\Psi_{1LH_1}^{0,s} + b\Psi_{1HH_1}^{0,d-} + c\Psi_{1HH_2}^{0,p+}. \quad (5)$$

It consists of s state of LH1, d_- state of HH1, and p^+ state of HH2. Here a, b, and c are the coefficients representing the contributions from different angular momentum components and will be determined by the quantum-well structures. The mixed exciton states in Eqs. (4) and (5) can be obtained by solving Eq. (3) using the techniques described in Ref. 15.

Substituting Eq. (4) or (5) into Eq. (3), we obtain the dipole moment of PI ISTs not only between the exciton states of same angular momentum such as s-s, p-p, and d-d (diagonal components) but also between the exciton states with different angular momenta such as s-p, p-s, s-d, and d-s (off-diagonal components). Such diagonal and nondiagonal components can happen simultaneously when a single infrared laser field near resonant with the transition between i and i' interacts with the QW structure. Compared to those considered previously, the non-s diagonal terms and the off-diagonal terms could lead to quite a different picture for the interaction of intense laser fields with quantum-well structures.

As studied in Refs. 11 and 12, the PI ISTs can be influenced by the dispersion of the valence subbands. In these references, however, this was studied considering s states of the excitons only. In this work, we will show how the valence-band structure affects PI ISTs through the mixed exciton states. The effects of the valence-band mixing on the exciton states have already been studied extensively.[14,15] Here, we only give a brief account to illustrate their impact on the PI ISTs.

Strong valence-band mixing is the precondition for exciton-state mixing to happen. At the band edge ($k=0$), there is no band mixing. Here one valence subband can be characterized by a single spinor index ν, i.e., the first heavy-hole subband (hh1) by $\nu=3/2$ and the first light-hole subband (lh1) by $\nu=-1/2$. Away from band edge, both $\nu=\pm 3/2$ and $\nu=\pm 1/2$ spinors will be present in one subband. The degree of mixing of different spinors will be determined by how close the subbands are. The subband positions are characterized by band-edge energies and can be effectively engineered through the introduction of strain by varying material composition.[17] To study the PI ISTs, we focus on subbands hh1 and lh1 and examine how they interact with each other and with hh2 and lh2. The band edge of these four subbands ($k=0$) of a 12-nm-wide $In_{1-x}Ga_xAs/InP$ QW are plotted as a function of Ga composition (x) in Fig. 2. Ga composition varies from 0.35 to 0.75, corresponding to compressive strain of 0.9% and tensile strain of 1.9%, respectively. (The range 0.35–0.75 is chosen for better illustration of the exciton mixing discussed in this work.) Figure 2 shows that three crossovers happen for hh1 and lh1. At $x=0.52$, hh1 (solid line) crosses over with lh1 (dashed line), at $x=0.68$ with lh2 (dotted line). At $x=0.47$, lh1 crosses over with hh2 (short dashed line). Strong valence-band mixings will happen around these crossovers.

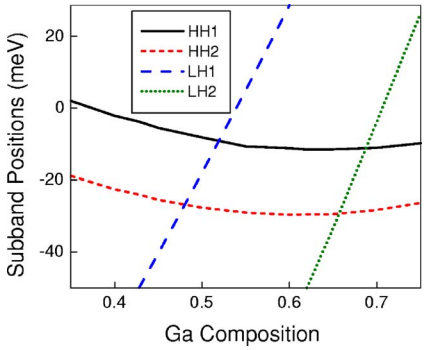

FIG. 2. (Color online) Subband positions of a 12-nm-wide $In_{1-x}Ga_xAs/InP$ quantum well for various Ga compositions.

To quantitatively study how such valence-band mixings influence the exciton states, we calculate the exciton-state mixing coefficients in Eqs. (4) and (5). The coefficients for the first state of $\xi=2$ and $i=1$ (Ψ_1^2) are plotted as function of Ga composition in Fig. 3(a). For x away from 0.68, the exciton state is mostly s state associated with hh1 subband, and around $x=0.68$, exciton states are a mixture of s state of hh1 (squares) and p^+ state of lh2 (filled circles). As shown in Fig. 2, $x=0.68$ is the crossover point of hh1 and lh2, demonstrating that strong exciton-state mixing occurs under the condition of strong valence-band mixing. It is also interesting to note that there is no exciton-state mixing around crossover $x=0.52$ even though a strong band mixing of hh1 and lh1 happens there. This is because the exciton-state mixing also requires the conservation of total angular momentum of exciton states (ξ). For the $\xi=2$ state, s state of hh1 cannot mix with any excitonic states of lh1 due to the angular momentum conservation. Similarly, the exciton-state mixing coefficients of the first state of $\xi=0$ and $i=1$ (Ψ_1^0) are calculated as a function of Ga composition and plotted in Fig. 3(b). For $x<0.47$ and $x>0.52$, the exciton states are primarily s states associated with lh1 (squares). Around $x=0.47$, exciton states are a strong mixture of s state of lh1 and p^+ state of hh2 (filled circles). At around $x=0.52$, exciton states are a strong mixture of s state of lh1 and d_- state of hh1 (filled triangles). Around 0.49–0.50, the center region between $x=0.47$ and $x=0.52$, the exciton states can be viewed as a mixture of s state of lh1, d_- state of hh1, d and p^+ states of hh2 although the last two components are small.

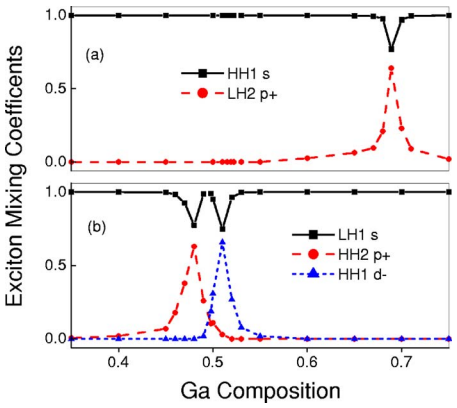

FIG. 3. (Color online) Exciton-state mixing coefficients: (a) $\xi=2$, $i=1$; (b) $\xi=0$, $i=1$.

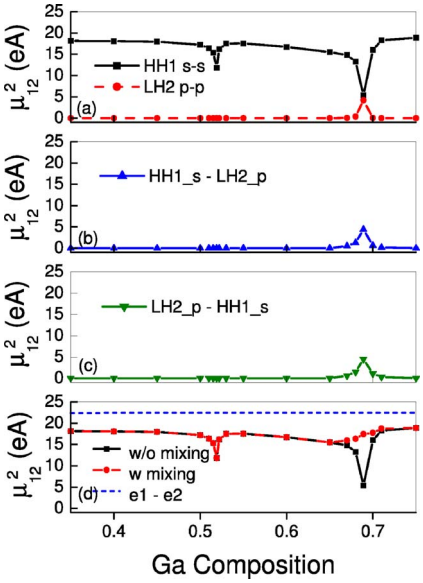

FIG. 4. (Color online) Dipole moments associated with the transitions between Ψ_1^2 and Ψ_2^2. (a) The s-s and p-p, (b) s-p, and (c) p-s transitions. (d) with and without exciton-state mixing.

To investigate the photoinduced conduction intersubband transitions under exciton-state mixing, the dipole moment contributions of various angular momentum components have been calculated for the 12-nm-wide $In_{1-x}Ga_xAs/InP$ QW. In Fig. 4, the dipole moments of PI ISTs from the first state of Ψ_1^2 to the first state of Ψ_2^2 are plotted as functions of Ga composition. Here, squares correspond to the s-s [Fig. 4(a)], circles to the p-p [Fig. 4(a)], up triangles to the s-p [Fig. 4(b)], and down triangles to the p-s transitions [Fig. 4(c)]. The overall dipole moments obtained from the models without and with exciton-state mixing are compared in Fig. 4(d). Here, squares correspond to that without exciton mixing, which is essentially the s-s transition in Fig. 4(a), and circles to that with exciton mixing, which is the summation of all angular momentum contributions. Away from $x=0.52$ and $x=0.68$, the dipole moment is primarily the contribution from s to s transition [see squares and circles in Fig. 4(d)]. At $x=0.52$ and $x=0.68$, the s-s transition is suppressed. This is because the strong valence-band mixings around these two points result in the reduction of $\nu=3/2$ components in hh1 that are associated with s states of e1-hh1 and e2-hh1. The suppression has been discussed in Ref. 12. However, our results show that, accompanying the suppression of s component at $x=0.68$, there are contributions from the p state and its cross terms with the s state. These transitions have not been previously accounted for and make up the loss of transition strength due to the reduction of the s component at this x composition. We can also notice that the non–s-s terms do not appear at $x=0.52$, because there is no mixing for the s states of exciton associated with hh1 due to the requirement of angular momentum conservation, as explained before. Finally, the dipole moments of the electron transitions between conduction subbands e1 and e2 are also plotted in Fig. 4(d) (dashed lines). Such transitions occur in n-doped QWs in the absence of photoexcited holes. We can see here that the exciton dipole moment is a little off from the electron dipole

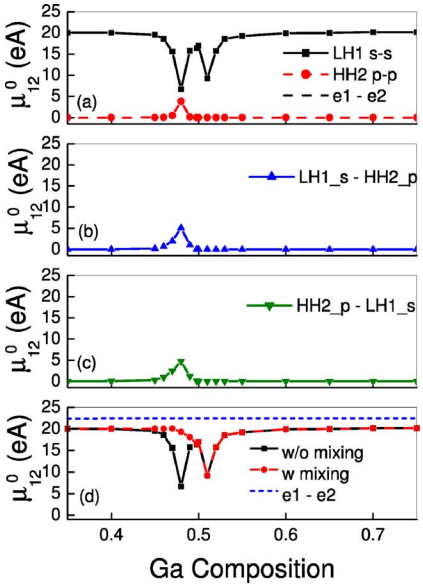

FIG. 5. (Color online) Dipole moments associated with the transitions between Ψ_1^0 and Ψ_2^0. (a) The *s-s* and *p-p*, (b) *s-p*, and (c) *p-s* transitions. (d) with and without exciton-state mixing.

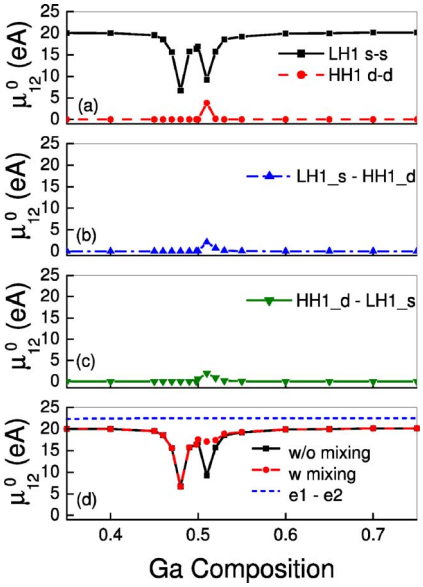

FIG. 6. (Color online) Dipole moments associated with the transitions between Ψ_1^0 and Ψ_2^0. (a) The *s-s* and *d-d*, (b) *s-d*, and (c) *d-s* transitions. (d) with and without exciton-state mixing.

moment in most regions. Around $x=0.52$, the PI IST strength will be significantly overestimated if the electron transition model is used.

The dipole moments of PI ISTs from the first state of Ψ_1^0 to the first state of Ψ_2^0 are plotted in Figs. 5 and 6 as a function of Ga composition. These figures show, respectively, the results of *s-p* and *s-d* mixing in the dipole moments of the PI ISTs. The comparisons between the dipole moments without and with exciton-state mixing are shown in Figs. 5(d) and 6(d). Similar to the case $\xi=2$ excitons, away from the two strong valence-band mixing points $x=0.47$ and $x=0.52$, the dipole moment has a contribution primarily from *s-s* transitions. At $x=0.47$, the *p-p*, *p-s*, and *s-p* transitions become significant, and at $x=0.52$, the *d-d*, *d-s*, and *s-d* transitions become significant. At $x=0.47$ and $x=0.52$, the model without exciton mixing will significantly underestimate the PI IST strength. The dipole moments of the electron transitions are also plotted in Figs. 5(d) and 6(d) (dashed line) for comparison.

In summary, we have shown that, when the exciton-state mixing occurs, an infrared laser near resonant with conduction subbands e1 and e2 can, in fact, lead to intersubband excitations with different angular momentum attributions. This may lead to a drastically different picture for the interaction of intense infrared lasers with QWs from that when no exciton effects or only *s* state excitons are considered. We have also shown that the dipole moments of PI ISTs could be drastically suppressed when strong valence-band mixing happens, but the exciton ground states remain pure *s* states. Our results also show that many of the drastic suppression previously predicted considering only the *s* states of excitons, however, will be compensated by the contributions of other orbital angular moments. The above results can have an impact on the way PI ISTs are being used to interpret physical processes in QWs. They can also be useful for the design of optical devices, where PI ISTs play a major role.

This work was supported in part by the Natural Sciences and Engineering Research Council of Canada through Agile All Photonic Network and in part by Ontario Research and Development Fund through Ontario Photonic Consortia.

[1] H. Schmidt and R. J. Ram, Appl. Phys. Lett. **76**, 3173 (2000).
[2] S. M. Sadeghi, S. R. Leffler, and J. Meyer, Phys. Rev. B **59**, 15388 (1999).
[3] M. D. Frogley, J. F. Dynes, M. Beck, J. Faist, and C. C. Phillips, Nat. Mater. **5**, 175 (2006).
[4] S. Butscher, J. Forstner, I. Waldmuller, and A. Knorr, Phys. Rev. B **72**, 045314 (2005).
[5] V. I. Klimov, J. Phys. Chem. B **110**, 16827 (2006).
[6] C. Gmachl, F. Capasso, D. L. Sivco, and A. Y. Cho, Rep. Prog. Phys. **64**, 1533 (2001).
[7] F. H. Julien, P. Vagos, J.-M. Lourtioz, D. Yang, and R. Planel, Appl. Phys. Lett. **59**, 2645 (1991).
[8] B. F. Levine, J. Appl. Phys. **74**, R1 (1993).
[9] M. Olszakier, E. Ehrenfreund, E. Cohen, J. Bajaj, and G. J. Sullivan, Phys. Rev. Lett. **62**, 2997 (1989).
[10] A. Neogi, H. Yoshida, T. Mozume, and O. Wada, Opt. Commun. **159**, 225 (1999).
[11] S. M. Sadeghi and W. Li, IEEE J. Quantum Electron. **40**, 343 (2004).
[12] S. M. Sadeghi and W. Li, Phys. Rev. B **70**, 195321 (2004).
[13] Jian-Bai Xia, Phys. Rev. B **40**, 8500 (1989).
[14] B. Zhu and K. Huang, Phys. Rev. B **36**, 8102 (1987).
[15] Calvin Yi-Ping Chao and S. L. Chuang, Phys. Rev. B **48**, 8210 (1993).
[16] L. C. Andreani and A. Pasquarello, Phys. Rev. B **42**, 8928 (1990).
[17] S. L. Chuang, Phys. Rev. B **43**, 9649 (1991).